An alternating direction implicit method for magnetohydrodynamic heat transfer in cylindrical geometry with discontinuity in wall temperature

B. Singh* and P. K. Agarwal†

The temperature distribution in the magnetohydrodynamic axial flow in a circular pipe has been found by using an alternating direction implicit method which has been suitably modified for r–θ–z geometry. First the temperature distribution far from the discontinuity, which ceases to depend upon the axial coordinate, has been found. This has been used to determine the results on both sides of the discontinuity. It is found that the temperature falls as the Hartmann number is increased, and convection dominates for large values of the Peclet number. The effect of the Hartmann number is more pronounced when Peclet number is large.

Keywords: *magnetohydrodynamics, heat transfer, alternating direction implicit methods*

Introduction

The study of magnetohydrodynamic (MHD) flow and heat transfer problems has become important due to several engineering applications in fields like MHD flowmetry, MHD power generation and in the design of cooling systems for nuclear reactors where liquid metals are used as coolants. Some simple MHD heat transfer problems like Hartmann flow between two parallel planes have been described by Sutton and Sherman[1]. As observed by them this simple one-dimensional problem becomes two-dimensional if wall temperature is discontinuous. Such problems offer many more difficulties for solution, as one can find in Nigam and Singh[2] who have considered heat transfer by laminar flow between parallel plates under the action of a transverse magnetic field.

In more practical situations such as MHD flow in a circular pipe the corresponding problem becomes three-dimensional, and only an efficient numerical method can be helpful in such cases. In the present paper an alternating direction implicit (ADI) method is described and used to find numerical results for the temperature distribution of MHD axial flow of a viscous incompressible and electrically conducting fluid in a straight, long circular pipe. The wall of the pipe has a temperature discontinuity at a section, on one side of which the temperature is T_1 and on the other side T_2 (see Fig 1). Owing to complex coupling of equations of electrodynamics and fluid mechanics, the resulting equations are fairly complicated and the exact analytical solution is out of the question.

The use of the ADI method in solving parabolic and elliptic equations in rectangular geometry is well known[3], but its use in polar coordinates, particularly when the singularity $r=0$ lies in the domain of interest, has appeared only very recently in connection with the solution of diffusion equation[4,5]. The aim of this paper is to extend the method to the energy equation in MHD which involves r, θ and z coordinates. The numerical results have been obtained for various values of the Hartmann number and Peclet number. Graphs and tables are given for the temperature distribution far from the discontinuity and also along the axis of the pipe. It is found that temperatures falls with increasing Hartmann number, and convection dominates as the Peclet number is increased.

Basic equations

The basic equations governing the steady flow of an incompressible, viscous and electrically conducting fluid in cylindrical coordinates (r', θ, z') in the presence of a transverse magnetic field are

$$\eta\nabla^2 V' + \frac{B_0}{\mu_0}\left(\cos\theta\frac{\partial B'}{\partial r'} - \frac{\sin\theta}{r'}\frac{\partial B'}{\partial\theta}\right) = -K \tag{1}$$

$$\lambda\nabla^2 B' + B_0\left(\cos\theta\frac{\partial V'}{\partial r'} - \frac{\sin\theta}{r'}\frac{\partial V'}{\partial\theta}\right) = 0 \tag{2}$$

$$k\left(\nabla^2 T' + \frac{\partial^2 T'}{\partial z'^2}\right) - \rho c V'\frac{\partial T'}{\partial z'} = \eta(\nabla V')^2 + \frac{1}{\mu_0^2\sigma}(\nabla B')^2 \tag{3}$$

* Department of Mathematics, University of Roorkee, Roorkee, 247667, Uttar Pradesh, India
† Regional Computer Centre, University of Roorkee, Roorkee, 247667, Uttar Pradesh, India
Manuscript received 23 January 1985 and accepted for publication on 31 October 1985

While deriving these equations, we have made the assumption that the flow is purely axial and the buoyancy forces caused by the temperature difference are negligible compared with the inertial and viscous forces. As a result of this assumption the velocity V' and the induced magnetic field B' are functions of r' and θ only, although the temperature T' depends on r', θ and z'. Such assumptions have been made by Nigam and Singh[2] for Hartmann flow, and Singh and Lal[6,7] for MHD flows between coaxial cylinders and through a rectangular pipe, respectively.

Let us introduce the dimensionless variables and parameters defined by

$$r=r'/a, \quad z=z'/a, \quad V_0=Ka^2/\eta$$
$$V=V'/V_0, \quad B=B'/V_0\mu_0(\sigma\eta)^{1/2}, \quad M^2=B_0^2a^2\sigma/\eta$$
$$T=(T'-T_2)/(T_1-T_2), \quad Q=V_0^2\eta/k(T_1-T_2),$$
$$P=\rho V_0 ac/k \tag{4}$$

Then Eq (1) to (3) are reduced to

$$V_{rr}+\frac{1}{r}V_r+\frac{1}{r^2}V_{\theta\theta}+M\left(\cos\theta\, B_r-\frac{\sin\theta}{r}B_\theta\right)=-1 \tag{5}$$

$$B_{rr}+\frac{1}{r}B_r+\frac{1}{r^2}B_{\theta\theta}+M\left(\cos\theta\, V_r-\frac{\sin\theta}{r}V_\theta\right)=0 \tag{6}$$

$$T_{rr}+\frac{1}{r}T_r+\frac{1}{r^2}T_{\theta\theta}+T_{zz}-PV(r,\theta)T_z=-Qf(r,\theta) \tag{7}$$

where

$$f(r,\theta)=V_r^2+\frac{1}{r^2}V_\theta^2+B_r^2+\frac{1}{r^2}B_\theta^2 \tag{8}$$

The exact solution of Eqs (4) and (5), subject to the boundary conditions

$$V(1,\theta)=B(1,\theta)=0 \tag{9}$$

which correspond to electrically non-conducting walls, has been found by Gold[8]. Singh and Lai[9] obtained numerical solution by using a finite element method. Gold's results are

$$V(r,\theta)=(u\,e^{-\alpha r\cos\theta}+v\,e^{\alpha r\cos\theta})/2 \tag{10}$$

$$B(r,\theta)=(u\,e^{-\alpha r\cos\theta}-v\,e^{\alpha r\cos\theta}-r\cos\theta/\alpha)/2 \tag{11}$$

where u, v are given by

$$u(r,\theta)=\frac{1}{2\alpha}\sum_{\omega=0}^{\infty}\varepsilon_\omega\frac{I'_\omega(\alpha)}{I_\omega(\alpha)}I_\omega(\alpha r)\cos\omega\theta \tag{12}$$

$$v(r,\theta)=\frac{1}{2\alpha}\sum_{\omega=0}^{\infty}(-1)^\omega\varepsilon_\omega\frac{I'_\omega(\alpha)}{I_\omega(\alpha)}I_\omega(\alpha r)\cos\omega\theta \tag{13}$$

with

$$\varepsilon_\omega=1 \quad \text{for } \omega=0$$
$$=2 \quad \text{for } \omega\geqslant 1 \tag{14}$$

The case $\alpha=0$ corresponds to the hydrodynamic Poiseuille flow. In this case the velocity field is independent of θ and is given by

$$V(r)=(1-r^2)/4 \tag{15}$$

The aim of the present paper is to determine the temperature distribution $T(r,\theta,z)$ from Eq (7) using the

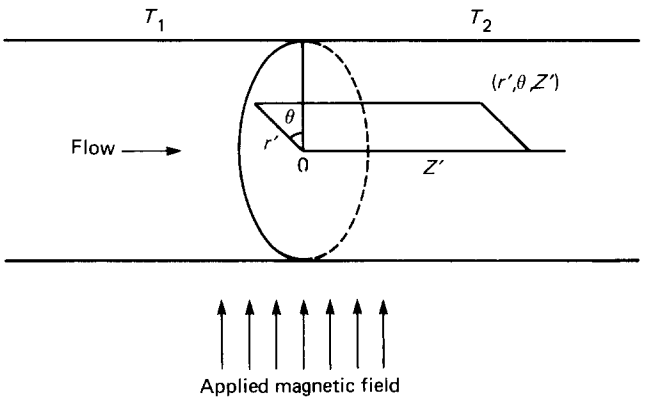

Fig 1 Geometry of system investigated

Notation

a	Radius of the pipe
b_i, c_i, h_i	See Eq (25)
B_0	Applied magnetic field
c	Specific heat of the fluid
c_{ij}, d_{ij}	See Eq (32)
h	Δr, the mesh size in the r-direction
I, J, K	See Eqs (22) and (28)
$I_\omega(\alpha)$	Modifined Bessel function
i, j, k	Suffixes used in r, θ, z directions
$-K$	Constant axial pressure gradient
k	Thermal conductivity of the fluid
M, P	Hartmann number, Peclet number
Q, V_0	Parameters defined in Eq (4)
r', θ, z'	Cylindrical coordinates
r_i, θ_j, z_k	See Eqs (2) and (28)
r, z, T	Dimensionless r', z' and T'
s	$h/\Delta z$
$T_{\pm\infty}$	Temperature as $z\rightarrow\pm\infty$
T_1, T_2	Wall temperature on the two sides of the discontinuity
T^n_{ijk}	Temperature at r_i, θ_j, z_k after n iterations
$T'(r',\theta,z')$	Temperature at (r',θ,z')
u, v	Defined in Eqs (12) and (13)
V, B	Dimensionless velocity and induced magnetic field
$V'(r',\theta)$	Axial velocity
$\Delta r, \Delta\theta, \Delta z$	Mesh size in r, θ, z directions
∇, ∇^2	Grad and div (grad) in polar coordinates (r',θ)
η	Coefficient of viscosity of the fluid
λ	Magnetic diffusivity $(\mu_0\sigma)^{-1}$
μ_0	A constant ($=4\pi\times10^{-7}$ in MKS system)
ρ	Density of the fluid
σ	Electric conductivity of the fluid
ϕ	Used for $T_{\pm\infty}$
ϕ^n_{ij}	Value of ϕ at r_i, θ_j after n iterations
ϕ_0	ϕ at $r=0$
ω	A parameter used to accelerate convergence

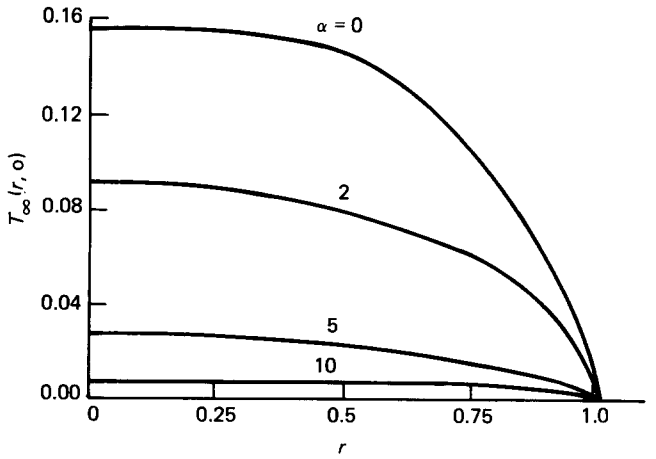

Fig 2 Radial temperature distribution for various values of α

above expressions for the velocity and induced magnetic field. The boundary conditions on T are

$$T(1,\theta,z)=1, \quad z<0$$
$$=0, \quad z>0 \quad 0\leqslant\theta\leqslant 2\pi \tag{16}$$

The other boundary conditions are provided by the temperature as $z\to\pm\infty$. Let us define

$$T_{\pm\infty}(r,\theta)=\lim_{z\to\pm\infty} T(r,\theta,z) \tag{17}$$

To obtain the differential equation satisfied by T_∞ and $T_{-\infty}$, we drop the terms involving partial derivatives of T with respect to z from Eq (7). This is due to the fact that as $z\to\pm\infty$, the perturbations in the temperature due to discontinuity at $z=0$ die out and so it ceases to depend upon z. Thus we get

$$\left(\frac{\partial^2}{\partial r^2}+\frac{1}{r}\frac{\partial}{\partial r}+\frac{1}{r^2}\frac{\partial^2}{\partial\theta^2}\right)T_{\pm\infty}=-Qf(r,\theta) \tag{18}$$

with boundary conditions

$$T_{-\infty}(1,\theta)=1, \quad T_\infty(1,\theta)=0, \quad 0\leqslant\theta\leqslant 2\pi \tag{19}$$

It is obvious that

$$T_{-\infty}(r,\theta)=1+T_\infty(r,\theta) \tag{20}$$

So we may find $T_\infty(r,\theta)$ only. The solution of Eq (18) is not possible in general. But for the hydrodynamic case $\partial/\partial\theta\equiv 0$ and $f(r,\theta)=r^2/4$ and so we get

$$T_\infty(r)=Q(1-r^4)/64 \quad (\textit{hydrodynamic case}, \alpha=0) \tag{21}$$

Solution as $z\to\pm\infty$

The analytical solution of Eq (18) subject to Eq (19) is not possible in closed form because the expression for $f(r,\theta)$ is very complicated. The usual finite difference method is also not suitable owing to the singularity at $r=0$. Further, to get reasonably accurate results a small mesh size has to be used. This leads to a large number of unknowns. So an appropriate method is the ADI method. For the diffusion equation in r–θ geometry it has been given by Evans and Gane[4,5]. This not only takes care of the singularity but also reduces the number of unknowns involved at a time, thus reducing the storage. The resulting equations along radial and transverse directions have simple structure for which efficient algorithms are available.

Let us introduce the finite difference mesh by defining

$$\Delta r=1/(I+0.5), \quad r_i=(i-1.5)\Delta r, \quad i=2(1)I+2$$
$$\Delta\theta=2\pi/J, \quad \theta_j=(j-1)\Delta\theta, \quad j=1(1)J \tag{22}$$

Denoting T_∞ by ϕ, the ADI equations for Eq (18) are as follows:

(i) For $j=1(1)J$

$$-b_i\phi^*_{i-1,j}+(\omega+2)\phi^*_{ij}-c_i\phi^*_{i+1,j}$$
$$=h_i^2(\phi^n_{i,j-1}+\phi^n_{i,j+1})+(\omega-2h_i^2)\phi^n_{ij}+Qh^2f_{ij},$$
$$i=2(1)I+1 \tag{23}$$

(ii) For $i=2(1)I+1$

$$-h_i^2\phi^{n+1}_{i,j-1}+(\omega+2h_i^2)\phi^{n+1}_{ij}-h_i^2\phi^{n+1}_{i,j+1}$$
$$=b_i\phi^*_{i-1,j}+(\omega-2)\phi^*_{ij}+c_i\phi^*_{i+1,j}+Qh^2f_{ij},$$
$$j=1(2)J \tag{24}$$

where

$$b_i=1-\frac{h}{2r_i}, \quad c_i=1+\frac{h}{2r_i}, \quad h=\Delta r, \quad h_i=h/(r_i\Delta\theta) \tag{25}$$

Notice that system (23) is a tridiagonal system with I unknowns for a fixed j. Since $b_2=0$, the value $\phi^*_{1,j}$ does not appear in (23). Also $\phi^*_{i+2,j}=0$ due to boundary conditions at $z=\infty$, since the coefficient matrix does not depend on j, we can have its LU-decomposition and use it for all values of j. Solving (23) for various values of j we get ϕ^* at all nodes in the section.

So far as the system (24) is concerned we notice that

$$\phi^{n+1}_{i,0}=\phi^{n+1}_{i,J} \quad \text{and} \quad \phi^{n+1}_{i,J+1}=\phi^{n+1}_{i,1}$$

and therefore it is not a tridiagonal system but a periodic tridiagonal system for which we use the algorithms given by Evans[10,11]. This will give ϕ^{n+1} at all nodes.

Thus by choosing the parameter ω suitably to have as fast a convergence as possible, and applying the above iterative process repeatedly, we obtain the temperature distribution in a section as $z\to\infty$. The temperatures for $z\to-\infty$ can then be obtained from Eq (20). To obtain results on the line $r=0$, it is not difficult to obtain the following interpolation formula:

$$\phi_0=\frac{1}{128J}\sum_{j=1}^{J}(315\phi_{2j}-420\phi_{3j}+378\phi_{4j}-180\phi_{5j}+35\phi_{6j}) \tag{26}$$

Computation of $T(r,\theta,z)$

Let us now return to the differential Eq (6) where the boundary conditions are provided by Eqs (16) and (17). In the previous section we have computed $T_\infty(r,\theta)$. From Eq (20) we then obtain $T_{-\infty}(r,\theta)$. As already remarked, the perturbations in T due to discontinuity in the boundary temperature at $z=0$ die out as we move on either side of $z=0$. Thus there exists a positive number Z such that the difference between $T(r,\theta,z)$ and $T_{\pm\infty}(r,\theta)$ is negligible for $|z|\geqslant Z$. A series of numerical experiments has been performed to estimate Z. Once it is known, the boundary conditions (17) may be replaced by

$$T(r,\theta,Z)=T_\infty(r,\theta)$$
$$T(r,\theta,-Z)=T_{-\infty}(r,\theta) \tag{27}$$

We thus have a Dirichlet problem in the domain $0 \leqslant r < 1$, $0 \leqslant \theta < 2\pi$, $-Z < z < Z$. Eq (7) is a three-dimensional elliptic equation with variable coefficients. Since analytic solution is out of the question, we use the ADI method for r–θ–z geometry. Defining the r–θ mesh by Eqs (22) and the mesh size in the z-direction by

$$\Delta z = 2Z/(K+1), \quad z_k = -Z + (k-1)\Delta z, \quad k = 1(1)K+2 \tag{28}$$

where there will be K internal nodes in the z-direction, the ADI equations are found to be

(i) For $j = 1(1)J$, $k = 2(1)K+1$

$$-b_i T^*_{i-1,jk} + (\omega+2)T^*_{ijk} - c_i T^*_{i+1,jk} = (\omega - 2h_i^2 - 2s^2)T^n_{ijk} + h_i^2(T^n_{i,j-1,k} + T^n_{i,j+1,k}) + c_{ij}T^n_{ij,k-1} + d_{ij}T^n_{ij,k+1} + Qh^2 f_{ij}$$
$$i = 2(1)I+1 \tag{29}$$

(ii) For $i = 2(1)I+1$, $k = 2(1)K+1$

$$-h_i^2 T^{**}_{i,j-1,k} + (\omega + 2h_i^2)T^{**}_{ijk} - h_i^2 T^{**}_{i,j+1,k} = (\omega - 2 - 2s^2)T^{**}_{ijk} + b_i T^*_{i-1,jk} + c_i T^*_{i+1,jk} + c_{ij}T^*_{ij,k-1} + d_{ij}T^*_{ij,k+1} + Qh^2 f_{ij}$$
$$j = 1(1)J \tag{30}$$

(iii) For $i = 2(1)I+1$, $j = 1(1)J$

$$-c_{ij}T^{n+1}_{ij,k-1} + (\omega + 2s^2)T^{n+1}_{ijk} - d_{ij}T^{n+1}_{ij,k+1} = (\omega - 2 - 2h_i^2)T^{**}_{ijk} + b_i T^{**}_{i-1,jk} + c_i T^{**}_{i+1,jk} + h_i^2(T^{**}_{i,j-1,k} + T^{**}_{i,j+1,k}) + Qh^2 f_{ij}$$
$$k = 2(1)K \tag{31}$$

where

$$c_{ij} = s^2 + 0.5PV_{ij}hs, \quad d_{ij} = s^2 - 0.5PV_{ij}hs \tag{32}$$

These are either tridiagonal or periodic tridiagonal systems and can be solved by the methods mentioned above.

Numerical results and discussion

The numerical work may be divided into the following parts.

(i) *Computation of* $f(r,\theta)$. To compute the numerical values of $f(r,\theta)$ at the mesh points in a section, Eqs (10) and (11) were differentiated and the derivatives of u and v substituted from Eqs (12) and (13). For this step, subroutines were prepared to compute I_ω and I'_ω. Due to shortage of space, these details and the numerical values are not given here.

(ii) *Computation of* $T_{\pm\infty}(r,\theta)$. This was done by using the method described above. Since it has not been possible to estimate theoretically the optimum value of ω as a function of Hartmann number and the mesh size, after a lot of experimentation it was found that for $I = 5$, $J = 16$, $Q = 1$, $\alpha = 0$ to 10, the optimum value is approximately 1.3. This gives stable results up to at least 6 significant digits in less than 50 iterations. For one value of α the CPU time on DEC-2050 was less than 10 s for 50 iterations. The iterations were started with zero initial values at all mesh points in the section. The values at $r = 0$ are found using Eq (26). We have given values of $T_\infty(r,\theta)$ at selected points for various values of α in Table 1.

(iii) *Computation of* $T(r,\theta,z)$. Here the computations are done for $I = 5$, $J = 16$, $K = 23$, $Q = 1$ for various values of α and P. After repeating the calculations for various values of Z it was found that for $|z| > 3$, the effect of z on T is negligible. So we have chosen $Z = 3$. The optimum value of ω was found to be approximately 1.5. About 40 iterations were required for the results to converge up to 6 significant digits. The CPU time on DEC-2050 was about 27 s for one value of α and P for 40 iterations. The starting values for iterations were taken as

$$\begin{aligned} T^\circ_{ijl} &= T_{-\infty}, & T^\circ_{ij,K+2} &= T_\infty \\ T^\circ_{ijk} &= 1.0, & -3 < z < 0 \\ &= 0.5, & z = 0 \\ &= 0, & 0 < z < 3 \end{aligned} \tag{33}$$

Due to the large number of variables and parameters involved, it is not possible to give here all the numerical results.

Table 2 gives the temperatures on the axis of the pipe for $\alpha = 0$, 2, 5, 10 and $P = 1$, 5, 10 and 20. From the results we make the following observations.

(i) As $z \to \infty$, the temperature distribution ceases to depend upon P as expected. From Table 1 and Fig 1 it can be seen that as α increases, the temperature decreases at all points in a section. Also the

Table 1 Values of $10\,T_\infty(r,\theta)$ for various α, r and θ
($w = 1.3$, $I = 5$, $J = 16$, $Q = 1$, 50 iterations)

α	θ	r						
		0	1/11	3/11	5/11	7/11	9/11	1.0
		$10\,T_\infty(r,\theta)$						
0	Arb	0.15625	0.15624	0.15539	0.14958	0.13063	0.08623	0.00000
2	0	0.09177	0.09203	0.08827	0.08124	0.07114	0.05331	0.00000
	$\pi/4$	0.09177	0.09215	0.08925	0.08311	0.07216	0.05067	0.00000
	$\pi/2$	0.09177	0.09227	0.09016	0.08460	0.07234	0.04751	0.00000
5	0	0.02813	0.02800	0.02635	0.02310	0.01847	0.01310	0.00000
	$\pi/4$	0.02813	0.02805	0.02681	0.02431	0.02047	0.01469	0.00000
	$\pi/2$	0.02813	0.02810	0.02721	0.02516	0.02134	0.01424	0.00000
10	0	0.00770	0.00767	0.00721	0.00627	0.00479	0.00268	0.00000
	$\pi/4$	0.00770	0.00766	0.00725	0.00642	0.00512	0.00328	0.00000
	$\pi/2$	0.00770	0.00766	0.00738	0.00680	0.00577	0.00393	0.00000

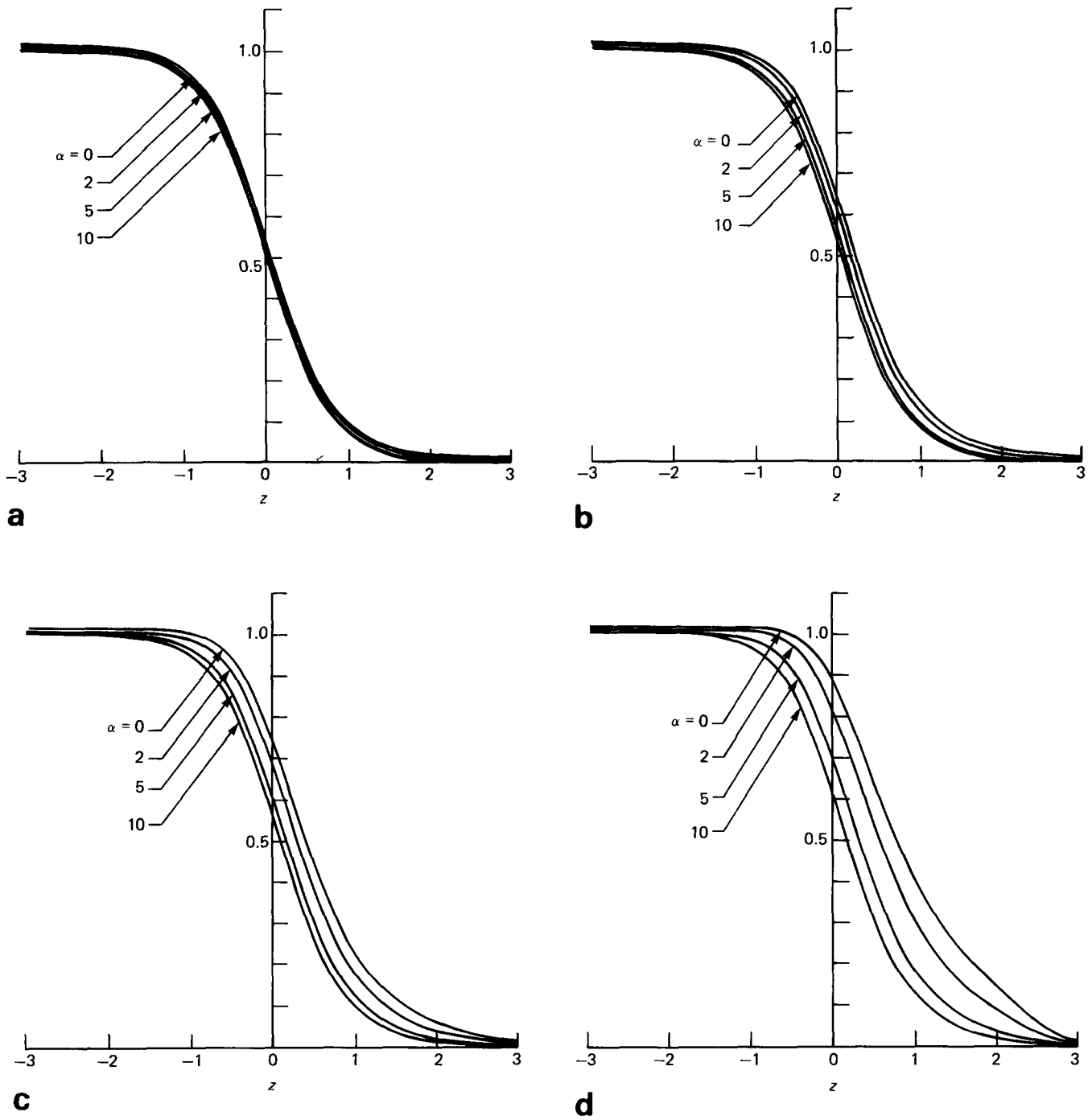

Fig 3 Axial temperature distribution for various values of α: (a) P = 1; (b) P = 5; (c) P = 10; (d) P = 20

temperature is maximum at $r=0$ and decreases to zero at the boundary.

(ii) Along a line parallel to the axis of the pipe the temperature decreases as we move from $z=-\infty$ to $z=\infty$. As this line moves closer to the wall, a sharp fall in temperature takes place as one moves across the section discontinuity in the wall temperature. This happens for all values of α and P for all lines. The temperature distribution along the axis of the pipe is given in Table 2.

(iii) As far as the effect of the parameter P (Peclet number) is concerned, we see from Figs 3(a)–(d) and Table 2 that, as P is increased, the effect of discontinuity in boundary temperatures continues up to longer distances. This is the well-known physical interpretation of the Peclet number. When P is large convection dominates conduction.

(iv) In the entire domain, increase in α results in decrease in temperature. Further, the effect of α is more pronounced when P is large, as is evident from Figs 3(a)–(d).

(v) We have not explicitly studied the effect of Q since it can always be absorbed in T, as can be seen from Eq (6). So, as Q is increased, T, will also increase in the same proportion. For all computations, Q has been chosen to be unity.

Table 2 Values of T on the axis of the pipe for various α, P and z

		z								
P	α	−3	−2	−1	−0.5	0	0.5	1	2	3
						T				
1	0	1.0156	1.0095	0.9533	0.8228	0.5400	0.2447	0.0956	0.0234	0.0156
	2	1.0092	1.0032	0.9441	0.8122	0.5276	0.2340	0.0886	0.0175	0.0092
	5	1.0028	0.9964	0.9348	0.7999	0.5131	0.2213	0.0789	0.0106	0.0028
	10	1.0008	0.9941	0.9310	0.7944	0.5064	0.2158	0.0750	0.0082	0.0008
5	0	1.0156	1.0130	0.9807	0.8864	0.6359	0.3280	0.1463	0.0348	0.0156
	2	1.0092	1.0064	0.9673	0.8620	0.6001	0.2947	0.1233	0.0248	0.0092
	5	1.0028	0.9985	0.9490	0.8292	0.5539	0.2541	0.0968	0.0140	0.0028
	10	1.0008	0.9954	0.9393	0.8110	0.5290	0.2334	0.0844	0.0099	0.0008
10	0	1.0156	1.0146	1.0008	0.9434	0.7426	0.4390	0.2243	0.0595	0.0156
	2	1.0092	1.0082	0.9866	0.9116	0.6847	0.3763	0.1766	0.0394	0.0092
	5	1.0028	1.0003	0.9636	0.8621	0.6039	0.2976	0.1225	0.0197	0.0028
	10	1.0008	0.9967	0.9486	0.8307	0.5570	0.2564	0.0972	0.0124	0.0008
20	0	1.0156	1.0151	1.0133	0.9976	0.8896	0.6398	0.4021	0.1465	0.0156
	2	1.0092	1.0091	1.0040	0.9721	0.8199	0.5377	0.3046	0.0904	0.0092
	5	1.0028	1.0021	0.9835	0.9149	0.6965	0.3892	0.1838	0.0372	0.0028
	10	1.0008	0.9985	0.9641	0.8662	0.6117	0.3046	0.1260	0.0190	0.0008

Acknowledgements

We are grateful to Dr S. C. Gupta and Dr M. N. Mahanta for their constant encouragement and valuable suggestions. We also thank Dr Jia Lal of Regional Computer Centre, Roorkee for helping us in computations.

References

1. **Sutton G. W. and Sherman A.** *Engineering Magnetohydrodynamics, McGraw-Hill, 1965*
2. **Nigam S. D. and Singh S. N.** Heat transfer by laminar flow between parallel plates under the action of a traverse magnetic field. *Quart. J. Mech. and Appl. Maths., 1960*, **13**, *85*
3. **Peaceman D. W. and Rachford H. H.** The numerical solutions of parabolic and elliptic equations. *J. Soc. Industr. Appl. Math., 1955*, **3**, *28*
4. **Evans D. J. and Gane C. R.** A.D.I. methods for the solution of transient heat conduction problems in r–θ geometry. *Int. J. Num. Meth. Eng., 1978*, **12**, *1799*
5. **Evans D. J. and Gane C. R.** A.D.I. methods for the solution of diffusion problems in r–θ geometry. *Comp. Meth. in Appl. Mech. Eng., 1982*, **31**, *281*
6. **Singh B. and Lal J.** Temperature distribution for MHD flow between coaxial cylinders with discontinuity in wall temperatures. *Appl. Sci. Res., 1979*, **35**, *67*
7. **Singh B. and Lal J.** Heat transfer for MHD flow through a rectangular pipe with discontinuity in wall temperatures. *Int. J. Heat Mass Transfer., 1982*, **25**, *1523*
8. **Gold R. R.** Magnetohydrodynamic pipe flow, pt. I. *J. Fluid Mech., 1962*, **13**, *505*
9. **Singh B. and Lal J.** Finite element method in magnetohydrodynamic channel flow problems. *Int. J. Num. Meth. Eng., 1982*, **18**, *1104*
10. **Evans D. J.** Direct methods of solution of partial differential equations with periodic boundary conditions. *Maths. and Computers in Simulation, 1979*, **21**, *270*
11. **Evans D. J. and Atkinson L. V.** An algorithm for the solution of general three-term linear systems. *The Computer Journal, 1970*, **13**, *323*